Rheology of a Miscible Polymer Blend at the Air−Water Interface. Quasielastic Surface Light Scattering Study and Analysis in Terms of Static and Dynamic Scaling Laws

Francisco Monroy,[†] Francisco Ortega, and Ramón G. Rubio*

Departamento de Química Física I, Facultad de Ciencias Químicas, Universidad Complutense, E-28040 Madrid, Spain

Received: June 9, 1998; In Final Form: October 9, 1998

Monolayers of poly(vinyl acetate) (PVAc) + poly(4-hydroxystyrene) (P4HS) blends on an aqueous subphase (pH = 2.0) have been studied over the whole surface concentration ($0 \leq \Gamma \leq$ collapse) and blend composition (mole fraction of PVAc $x_1 = 0-1$) ranges. Besides a classical surface tension technique, a surface light scattering by thermally excited capillary waves spectrometer has been used. The results obtained include the static surface pressure Π and elasticity ϵ_{st}, as well as the dynamic dilatational elasticity $\epsilon_0(\omega)$ and viscosity $\kappa(\omega)$ as a function of frequency ω. The analysis of the Π vs Γ curves point out that the aqueous−air interface behaves as a good solvent for the monolayers of PVAc-rich blends, while it is a near-Θ solvent for P4HS-rich blends. The critical exponent ν calculated from the static results in the semidilute regime is in excellent agreement with the values obtained from $\kappa(\omega)$ for all the samples. The relaxation times obtained from the dynamic data are compatible with the description of the monolayers as 2-D gel-like systems. In the concentrated regime it is found that $\epsilon_{st} > \epsilon_0$, which suggests the existence of diffusive processes out of the plane of the interface.

1. Introduction

For several decades, the rheology of 3-D polymer melts has been studied both theoretically and experimentally.[1] On the basis of scaling hypotheses, de Gennes has developed a theory for the dynamics of entangled polymer solutions in the case of an arbitrary space dimensionality d.[2] This theory, which assumes Rouse-type dynamics for individual chains plus a collective reptation,[3,4] relies on the existence of a correlation length ξ which depends on the polymer concentration, and it is independent of the molecular mass M_w. ξ can be conceived as the distance between entanglement points; while in 3-D, ξ is inversely proportional to the osmotic pressure, in 2-D (monolayers), ξ is inversely proportional to the surface pressure Π.[2] De Gennes' theory has been extensively tested for 3-D systems,[5] and the scaling laws have been found to describe very accurately the static results of surface pressure Π and elasticity coefficient ϵ_{st} in quasibidimensional polymer monolayers. However, there is much less information about the rheology of the polymer monolayers.[6] The description of the behavior of static properties, such as Π and the static elasticity modulus ϵ_{st}, and of dynamic properties such as the frequency dependent elastic modulus ϵ_0 and dilational viscosity κ can be done in terms of a few variables: ξ, the critical exponent ν, etc. The main aim of the present work is the comparison of the critical exponents obtained from both static and dynamic properties of the same systems, which will constitute a strong test of the theory.

The rest of the paper is organized as follows. Section 2 provides some background on the theory behind the description of the capillary waves. Section 3 summarizes the experimental details, and section 4 gives the results, which are discussed in section 5. Finally, section 6 gives the main conclusions.

2. Theoretical Background

Liquid interfaces are continuously perturbed by random thermal fluctuations of energy k_BT, which can be considered as a dynamic roughness and may be rationalized by decomposing these fluctuations as an infinite series of discrete Fourier modes. If this fluid interface is constituted by a polymer film, we can treat it in the limit $qR_F < 1$ as if it was a viscoelastic continuum medium,[7] with R_F (the "Flory radius") being the radius of an isolated polymer coil in the presence of excluded volume effects, which gives an idea of the molecular dimensions in the monolayer.[8] This limit corresponds to values of the characteristic experimental wavelength $\lambda = 2\pi/q$, being very long when compared with the molecular dimensions, usually known as the hydrodynamic limit.

2.a. Surface Modes and Dispersion Equation. In this space scale (10^{-6} to 10^{-5} m), the hydrodynamic motion in the polymer film can be decomposed in two main modes, capillary (or out of plane) and longitudinal (or in plane);[9,10] however, other modes (splay and bending) exist associated with fluctuations in the molecular director, which are fully uncoupled from these main motions.[11] Moreover, the capillary mode, which produces strong fluctuations in the dielectric constant at the surface, is responsible for the light scattered by the interface. This mode is essentially a shear motion, governed by surface tension γ and gravity g, which may be seen as restoring forces in the perpendicular direction to the film plane. The longitudinal mode must be decomposed in both a compression and a shear motion characterized by two different elastic moduli (K and S, respectively). Since dissipative effects do exist within the film, each one of these uniaxial motions are governed by a set of

* To whom correspondence should be addressed. E-mail: rgrubio@eucmax.sim.ucm.es.

[†] Current address: Laboratoire de Physique des Solides, Bât. 510, University Paris-Sud, 91405 Orsay, France.

10.1021/jp982548m CCC: $18.00
Published on Web 03/05/1999

viscoelastic response functions, which can be written as[9,12]

$$\tilde{\gamma}(\omega) = \gamma_0 + i\omega\mu \quad (1)$$

$$\tilde{\epsilon}_K(\omega) = K + i\omega\eta_K \qquad \tilde{\epsilon}_s(\omega) = S + i\omega\eta_s \qquad \tilde{\epsilon}(\omega) = \tilde{\epsilon}_K(\omega) + \tilde{\epsilon}_s(\omega) = \epsilon_0 + i\omega\kappa \quad (2)$$

Equation 1 holds for capillary and eq 2 for longitudinal motions, respectively, where ω denotes the angular frequency.

The imaginary parts of each of these viscoelastic moduli are the loss components, characterized by the viscosity coefficients μ, η_K, η_S, each one of them leads to viscous dissipation in the *XZ* and *XY* planes. If classical elasticity for a 2D homogeneous medium is considered, pure compression and shear components appear mixed in the stress response to an in-plane uniaxial strain, as is the case for a surface plane wave.[7,10] Therefore, one can define a total longitudinal viscoelastic modulus as the sum of the compression and shear moduli, defined by a real part or *dilational elasticity* ϵ_0 and a dissipative term or *dilational viscosity* κ. The shear contribution S to dilational elasticity will be different from zero only for solid films, where the dislocations and defects accumulate elastic energy.[7,13] Also, the shear contribution to dilational viscosity, η_S, although in general presents nonzero values, is several orders of magnitude smaller than the compression component η_K.[14] Therefore, the compressional properties, denominated *per extension dilational viscoelasticity*, are generally accepted as the dominant properties in interfacial hydrodynamics.[15] The real existence of the transversal viscosity μ has been often questioned. As it was suggested by Goodrich in his seminal work in surface mechanics,[12,16] the dissipation in the transversal motion must arise from differences in the molecular tilt when the transversal wave passes perturbing the equilibrium homogeneous tilt distribution. Therefore, the transversal dissipative effects might give more appreciable contributions at high frequency.[16] Recently, Kikuchi et al.[17] have experimentally evidenced the nonexistence of this contribution for the free surface of liquids, at least at frequencies up 10 MHz. Only for very dense insoluble monolayers, the transverse shear viscosity μ, might give appreciable contributions.[16,18] Particularly, previous studies on concentrated phospholipid bilayers[19] and on monolayers of pure PVAc[18] have found that this transversal viscosity presents comparable values to the dilational one, but in both cases, the first motion relaxes more rapidly than the dilational or in-plane motion, normally at frequencies higher than 100 kHz. Therefore, for a given monolayer at the frequencies considered here, 50 kHz typically, and if a Maxwell-like viscoelastic response is assumed,[20] the transversal motion can be considered fully relaxed, with γ_0 being essentially independent of frequency and equal to the equilibrium thermodynamic value, while $\mu(\omega)$ will also be a constant quantity, corresponding to the Newtonian limit of the transversal viscosity, $\mu = \mu(\omega \rightarrow 0)$.

In a very recent work, Buzza et al.[21] have developed a theory for surface light scattering from a fluid−fluid interface with adsorbed polymers. In contrast to current phenomenological models,[16−18] they showed that there is no viscous counterpart for the transversal elastic modulus, i.e., $\mu = 0$. They also found that for thick monolayers (e.g., adsorbed polymeric surfactants) two additional surface moduli (the bending and the coupling moduli) are necessary for a complete description of the viscoelastic behavior of the interface. The polymers used in the present work form insoluble monolayers, hence one must expect the bending and coupling contributions to be negligible.[21]

The solution to the hydrodynamic problem of a liquid surface with such viscoelastic films spread on it has been frequently discussed in the bibliography.[10,16,22] In brief, when the hydrodynamic Navier−Stokes equations for oscillatory motion in the form given by eq 3 are solved at the air−fluid interface together with the appropriate interfacial limit conditions,

$$\mathbf{u}_q(\mathbf{r},t) = \sum_q \mathbf{u}_q^{(0)} e^{i(qr+\omega t)+mz} \quad (3)$$

it can be found capillary and dilational modes coupled together. The dispersion equation, $D(\omega)$, for this coupled motion finally is written

$$D(\omega) = LT - [i\omega\eta(q-m)]^2 = 0 \quad (4)$$

where

$$L = \tilde{\epsilon}q^2 + i\omega\eta(q+m) \text{ and } T = \tilde{\gamma}q^2 + i\omega\eta(q+m) - \frac{\rho}{q}\omega^2 + \rho g \quad (5)$$

with ρ and η being the liquid density and viscosity, respectively, and m^{-1} is known as the *capillary penetration length*, which gives us a measurement of the damping of the surface velocity field in the liquid. This parameter is given by

$$m^2 = q^2 + i\omega\frac{\rho}{\eta} \quad \text{with} \quad \mathrm{Re}(m) > 0 \quad (6)$$

Equations 4 and 5 point out that capillary and dilational motions are coupled at air−liquid interfaces. This coupling is the physical mechanism which allows us to measure dilational properties by means of capillary waves devices, such as light scattering from capillary waves. The only condition for uncoupling at the air−liquid interface is the limit $m \rightarrow q$, which is fulfilled at very low frequencies or at very large liquid viscosities. This is not the case for thermally excited capillary waves at air−water interfaces. This coupling is maximum when the frequencies of capillary and dilational waves are equal, i.e., at resonance. Experimentally, this point will be easily observable as a noticeable increase in the damping coefficients of the surface modes.[16] This resonance condition is slightly ω dependent and for our systems corresponds at values of $\epsilon_0/\gamma_0 \approx 0.1-0.2$ depending on frequency. The maximum sensitivity of our capillary waves device is found at any point in this range.

2.b. Light Scattering. Light scattering from thermally excited capillary waves is actually one of the most convenient of the available techniques for studying surface viscoelasticity. The frequency ω of a capillary mode is a complex quantity which contains as the real part the angular velocity or oscillation frequency ω_0 and the imaginary damping constant Φ, which leads to decay time of the mode,

$$\omega = \omega_0 + i\Phi \quad (7)$$

Because of the propagative nature of capillary waves, these surface modes scatter light at frequency ω_0 and with spectral broadening proportional to Φ. The power spectrum $P(\omega)$ of the scattered intensity is given by the following expression, which depends on both dilational and capillary parameters:

$$P(\omega) = -\left(\frac{k_B T}{\pi\omega}\right)\mathrm{IM}\left[\frac{\epsilon q^2 + i\omega\eta(q+m)}{D(\omega)}\right] \quad (8)$$

The Fourier transform of $P(\omega)$ gives the corresponding autocorrelation function $g(\tau)$, which contains exactly the same information in the temporal domain. In the case of the scattered

light by capillary modes at the air−water interface, the spectral profile may be approximated by a Lorentzian shape,[10,16] resulting in a damped sinusoid as the approximated expression for the autocorrelation function:

$$g(\tau) \approx \cos(\omega_0 \tau) e^{-\Phi \tau} \tag{9}$$

These propagation parameters ω_0 and Φ are directly related to the solutions of the dispersion equation given in eqs 4−6 when $y \gg 1$ $((\gamma\rho)/(4\eta^2 q))$, obtaining, in the case of $\epsilon = \omega\kappa = 0$ and $\eta \rightarrow 0$ limit, the following zero-order solution for the capillary mode:

$$\omega_C^{(0)} = \omega_0 + i\Phi_0 \approx \left(\frac{\gamma}{\rho} q^3\right)^{1/2} + 2i\frac{\eta}{\rho} q^2 \tag{10}$$

The real capillary motion of viscoelastic films generally is not governed by this ideal limit solution, but it can be considered as a first approximation to propagation parameters. By supposing that the zero-order formula given in eq 10 is valid for transversal motion, Earnshaw et al.[21] have calculated an estimation for the maximum value of the transversal viscosity μ compatible with the observed damping Φ_{Exp}.

$$\Delta\Phi = \Phi_{Exp} - \Phi_0 \approx \frac{\mu_{max}}{2\rho} q^3 \approx \frac{\mu_{max}}{2\gamma_0} \omega_0^2 \tag{11}$$

It must be stressed that such an estimation is valid only as far as the Kelvin solution of the dispersion equation is satisfactory.

3. Experimental Section

3.a. Chemicals. Polymers were purchased from Polysciences (Germany) and used as received. Poly(vinyl acetate) had a weight-average molecular weight $M_w = 90000$, and for poly(4-hydroxystyrene), $M_w = 10000$. In both cases, the polydispersity indexes were approximately 1.3. We checked by UV and ^{13}C NMR that no significant amount of the hydroxyl groups of P4HS had reacted to the quinone form.

The spreading solutions were a mixture of tetrahydrofurane + benzene (10:1) and had a concentration close to 10^{-3} M. The solvents were purchased from Carlo Erba (RPE quality). Before preparing the polymer solutions, the surface tensions of solvents were measured by the plate method in order to ensure that they did not have significant amounts of surface-active impurities. Good agreement was found between the values measured and those reported by Jasper.[24] Before the spreading solution was prepared, the pure polymers were dissolved in tetrahydrofurane and filtered through 0.5 μm Teflon membranes. Different amounts of these solutions of each polymer were mixed to prepare the blend polymer solutions. Double distilled and deionized water from a Milli-Q-RG system was used. Its resistivity was always higher than 18 MΩ cm^{-1}. The subphase of pH = 2, needed to prevent hydrolysis of the functional group of P4HS, was obtained by adding HCl solution (Carlo Erba).

3.b. Langmuir Trough. The monolayers were formed on a commercially available Teflon Langmuir trough (KSV Instruments model 3000 with a minitrough, Finland). A Pt−Wilhelmy balance was used as a surface pressure sensor. Polyoxymethylene (Delrin) hydrophilic barriers were used. The whole setup was enclosed in a box made of transparent methacrylate through which a small flow of filtered N_2 was maintained. A Petry cell with subphase was placed inside the box in order to keep the humidity at saturation level. The temperature control in the trough was carried out by passing thermostated water into the jacket at the bottom of the trough. The temperature near the surface was measured with a calibrated Pt-100 sensor. The temperature of the box was maintained constant within ±0.1 degrees at the same temperature as the measurements. The box has two optical windows for the light scattering experiments. The surface of the subphase was swept with the barriers until the expected surface tension was obtained. To ensure that the spreading solvent did not add any significant impurities, blank experiments with the pure solvent were done before forming a monolayer.

To form the monolayers, small amounts of the spreading solutions (typically 25 μL) were slowly applied by a microsyringe (Hamilton) at different places on the surface. The surface concentration was changed by subsequent additions of the polymer solution. Times ranging from 15 to 50 min were allowed for solvent evaporation and monolayer equilibration. The surface pressure, Π, was continuously monitored, and the equilibrium value was taken only when Π remained constant for at least 20 min.

Each reading of the surface tension was determined with ±10 μN m^{-1}, although the repetitivity under small cyclic changes of the position of the barriers was around 3 times greater, with the absolute uncertainty being around ±30 μN m^{-1}. The stability of the subphase temperature was better than ±0.1 degrees. All the experiments were performed at a constant temperature of 25.0 ± 0.1 °C.

3.c. Surface Light Scattering Experiments. The surface light scattering spectrometer used here is similar to the one described by the groups of Earnshaw and McGiven,[23] Richards et al.,[25] and Yoo and Yu,[26] and it has been described elsewhere.[18] Briefly, a polarized 25 mW He−Ne laser passes a diffraction gratting and then a focusing lens, which forms a 1:1 image of the gratting on the monolayer. The light scattered by thermally excited capillary waves is detected in the heterodyne mode, mixed with the light corresponding to a diffraction order reflected by the surface and with wave vector q. Each of them is focused in the photomultiplier, and its output signal is collected and analyzed by a NICOMP 170 autocorrelator. The experimental autocorrelation functions are described as the convolution of the theoretical $g(\tau)$ given in eq 9 and instrumental contributions, fundamentally derived from the finite size of the laser spot in the detector plane. The experimental $g(\tau)$ finally is given by[27]

$$g_{Exp}(\tau) = A\cos(\omega_0\tau + \varphi)e^{-\Phi\tau}e^{-(\beta\tau/2)^2} + A_f e^{-\Theta_f\tau} + B - C\tau^2 \tag{12}$$

The term $D\tau^2$ accounts for the influence of possible long-wavelength contributions from building vibrations, while $A_f \exp(-\Theta_f\tau)$ for after pulsing effects at $\tau \leq 5$ μs; however, both terms have been usually negligible in the frequency range considered here. The instrumental effects from the finite size of the laser beam on the photomultiplier are accounted for by the Gaussian term $A \exp[-(\beta\tau/2)^2]$. The exponentially damped cosine theoretical term incorporates the damping Φ and the frequency ω_0 of the capillary waves. A phase factor φ is included to accommodate the experimental observation that the power spectrum is in general a skewed Lorentzian. This spectrometer has been calibrated using simple liquids (*n*-hexane, ethanol, and water) and can be used in the wave vector range $100 \leq q$ (cm^{-1}) ≤ 900.

4. Experimental Results

4.a. Static. The equilibrium properties of the PVAc + P4HS system have been discussed in detail in a previous work.[28] Here,

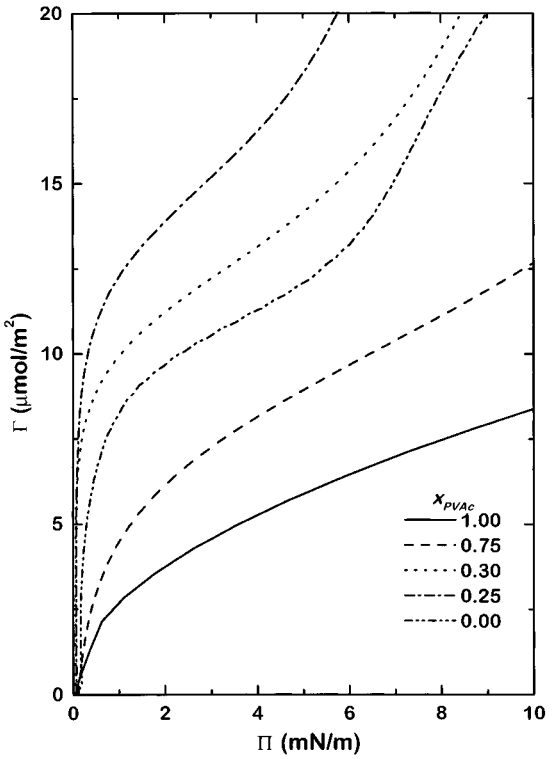

Figure 1. Surface concentration Γ vs surface pressure Π curves for the monolayers of the x_1 PVAc + $(1 - x_1)$ P4HS blend at 25 °C and for some selected weight fractions of PVAc x_1 as indicated.

we will show some of the data that will be used below in discussing the dynamic results. Figure 1 shows some of the Γ−Π curves at 25 °C as a function of the composition of the blend. While the PVAc monolayer is of the expanded type, P4HS forms a compressed-type monolayer. It is worth noting that small amounts of P4HS in the blend make the monolayers of the compressed type, with this effect being maximum for the blend close to 75% in weight of P4HS. The analysis of the excess Gibbs energy confirms that the two polymers form miscible blends in the monolayer state over the whole composition range.[28]

Figure 2 shows the static compressibility coefficient ϵ_{st} for the two pure polymers and for the blend with 25% in PVAc.

$$\epsilon_{st} = \lim_{\omega \to 0} \tilde{\epsilon}(\omega) = \left(\frac{\partial \Pi}{\partial \ln \Gamma}\right)_T \qquad (13)$$

As expected, ϵ_{st} increases in the semidilute regime of the monolayer (see Discussion). The value of the maximum of ϵ_{st} decreases with the expanded character of the monolayer. It must be noticed that for P4HS ϵ_{st} shows an anomalous behavior, since after the maximum, it increases again at high surface concentrations. This behavior has already been found for poly(phenylsiloxane)[29] and blends of PVAc and poly(dimethylsiloxane).[30] It has been related to the existence of order and/or packing transitions when the monolayers are compressed.

4.b. Capillary Wave Frequency and Damping. We have measured the correlation functions at $q = 344.4$ cm^{-1} for eight values of the molar fraction of the blend x_1 and from low values of the surface concentration up to the collapse pressure. Figure 3a shows two representative autocorrelation functions, one obtained at surface concentration $\Gamma = 8$ μmol m^{-2} and $x_1 = 1.0$, and the other one at $\Gamma = 13$ μmol m^{-2} and $x_1 = 0.25$, when the resonance condition is fulfilled and the capillary damping becomes maximum. This figure shows a strong

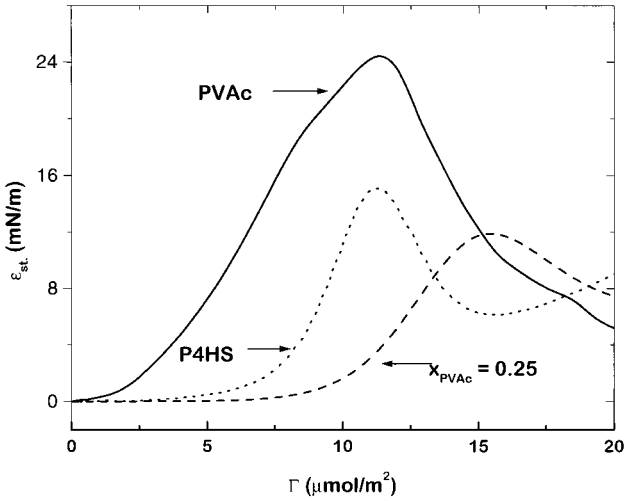

Figure 2. Static elasticity modulus for the pure polymer monolayers and for the blends with 25% of PVAc. Other blend compositions have been omitted for the sake of clarity.

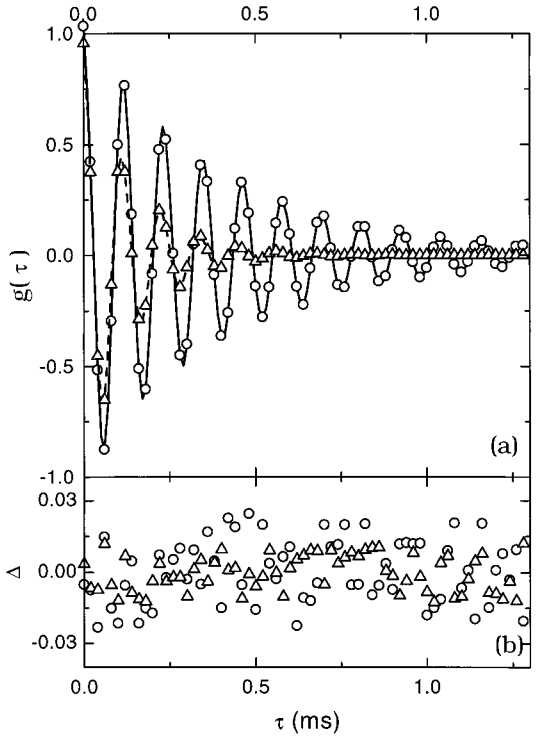

Figure 3. (a) Representative normalized heterodyne correlation functions and their fits to eq 12: (○) $\Gamma = 8$ μmol m^{-2} and $x_1 = 1.0$; (△) $\Gamma = 13$ μmol m^{-2} and $x_1 = 0.25$. (b) Differences between the experimental correlation functions and the fits to eq 12 (symbols as in (a)).

increase in the damping of the autocorrelation function and a weak variation in its oscillation frequency. Both the frequency and the damping have been obtained from fits of the correlation functions to eq 12. Figure 3b shows that the residuals are randomly distributed; similar results were obtained for the other correlation functions. Figure 4 shows the results for three of the blends. As expected, the reduced frequency and damping extrapolate to the ideal limit behavior $\omega^* \to 1$, $\Phi^* \to 1$ at $\Gamma \to 0$, where $\omega^* = \omega(q)/\omega_0$ and $\Phi^* = \Phi(q)/\Phi_0$, with ω_0 and Φ_0 given in eq 10. In the dilute and semidilute regimes, ω^* and the propagation velocity of the transversal mode $c_T = \omega_0 q^{-1}$, grow with Γ, which correlates well with the increase of ϵ_{st} in that surface concentration range. The value of Γ at which the maximum of ω^* occurs is found to be close to (slightly lower

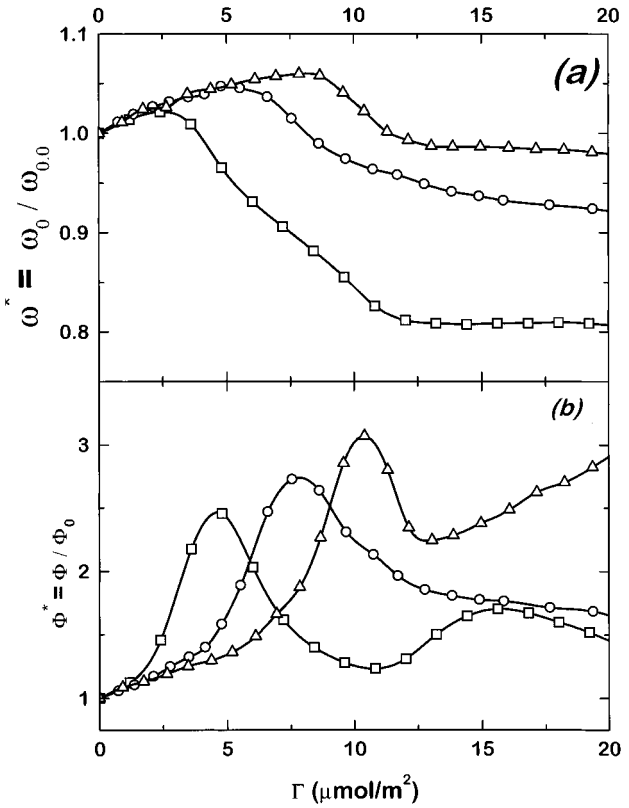

Figure 4. (a) Reduced frequency, ω^*, and (b) reduced damping, Φ^*, of the capillary modes of polymer monolayers for three different values of x_1: (□) 1.0; (○) 0.75; (△) 0.25. The value of the wave vector is q = 344.4 cm^{-1}. The reducing parameters used the values corresponding to the limit ideal solutions (eq 10), which for our value of q are ω_0 = 54.66 kHz and Φ_0 = 2.13 kHz. The error bars have been omitted because they are comparable to the points size.

than) the maximum of the damping curves (Figure 4b), which can be understood in terms of the resonance of the capillary and longitudinal modes of the interface. As Γ is increased further, ω^* decreases, with the magnitude of the decrease being larger for the more expanded isotherms. For Γ > 12 μmol m^{-2}, ω^* becomes independent of the surface concentration.

The value of Γ for which Φ^* is maximum can also be understood in terms of the values of ϵ_{st}. In effect, this concentration increases as the content of PVAc in the blend decreases, i.e., as ϵ_{st} for a given Γ decreases. This behavior can be rationalized in terms of the zero-order formula, eq 10, for capillary modes and the approximate dispersion equation for the dilational modes given by Lucassen and van den Tempel,[31]

$$\omega_L^{(0)} \approx \frac{\sqrt{3}+i}{2}\left(\frac{\epsilon^2 q^4}{\eta\rho}\right)^{1/3} \qquad (14)$$

from which the following resonance condition can be obtained:

$$\alpha = \frac{\epsilon_0}{\gamma_0} = \left(\frac{q\eta^2}{\gamma\rho}\right)^{1/4} \approx 0.1-0.2 \qquad (15)$$

Figure 5 shows the values of α calculated from the Π−Γ curves for the values of Γ for which the maxima of the Φ^* vs Γ appear for the different blends. The agreement with eq 15 is excellent, confirming that the resonance in this systems is established via the condition $\omega_C = \omega_L$, where subscripts C and L refer to capillary and longitudinal, respectively.

4.c. Surface Viscoelasticity. Several methods have been followed in the literature in order to obtain the four viscoelastic

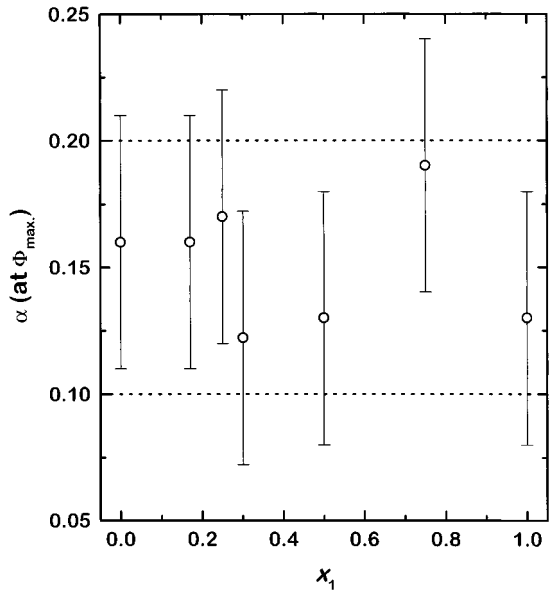

Figure 5. Elasticity ratio $\alpha = \epsilon_0/\gamma_0$ at the surface composition for which the damping takes the maximum value. The dotted lines represent the limits for the theoretical condition of resonance of the capillary modes (eq 15).

parameters from the light-scattering data. Kawaguchi et al.[32] assumed $\gamma_0 = \gamma_{st}$, the later being the surface tension measured by classical static methods, and $\mu = 0$. The values of ϵ_0 and κ were then obtained from the frequency and the width of the spectrum $P(\omega)$ (eq 8). In a later work, Yoo and Yu[26] assumed that for their polymer monolayers ϵ_0 and κ should be almost independent of q and solved the dispersion equation under this constraint. Although this method led to $\mu \neq 0$, the numerical values of ϵ_0 and κ were quite similar to those obtained assuming $\mu = 0$. However, in a recent work[18] we have found that for monolayers of pure PVAc, both ϵ_0 and κ were frequency dependent in the kHz range explored with our technique.

Earnshaw et al.[33] have discussed in detail how to obtain γ_0, μ, ϵ_0, and κ from the experimental correlation functions by fitting them to the Fourier transform of the theoretical spectrum. The success of the method relies mainly in the departure of the experimental spectrum from a pure Lorentzian shape. This method has been considered to be the only one adequate for monolayers of soluble polymers and for monolayers that show phase transitions, in which negative values of the viscosities are frequently found.[27,34,35]

Detailed analysis of the different terms of the dispersion equation has led to useful conclusions about the conditions under which the elastic and viscous coefficients of the transverse and dilatational modes can be best determined from QESLS experiments. From eq 10 it is γ_0 which has the most significant influence on the frequency of the capillary waves.[19] The damping of the capillary waves is influenced by dilatational properties because of the coupling of dilatational and capillary waves. Notwithstanding this coupling, the major factor influencing the damping is μ.[33] The increase of the damping is, to first order, $\Delta\Phi = \mu q^3/(2\rho)$ so that light scattering becomes increasingly sensitive to μ as q is rised.[19] The q value used in this work, q = 344.4 cm^{-1}, is not large, which makes hard a precise determination of μ. A similar situation has been described previously by Earnshaw et al.[19] On the other hand, the use of small values of q is desirable due to the decreasing influence of ϵ_0 and κ on the capillary waves as the momentum transfer, q, parallel to the surface increases.[18] Richards et al.[24] have also

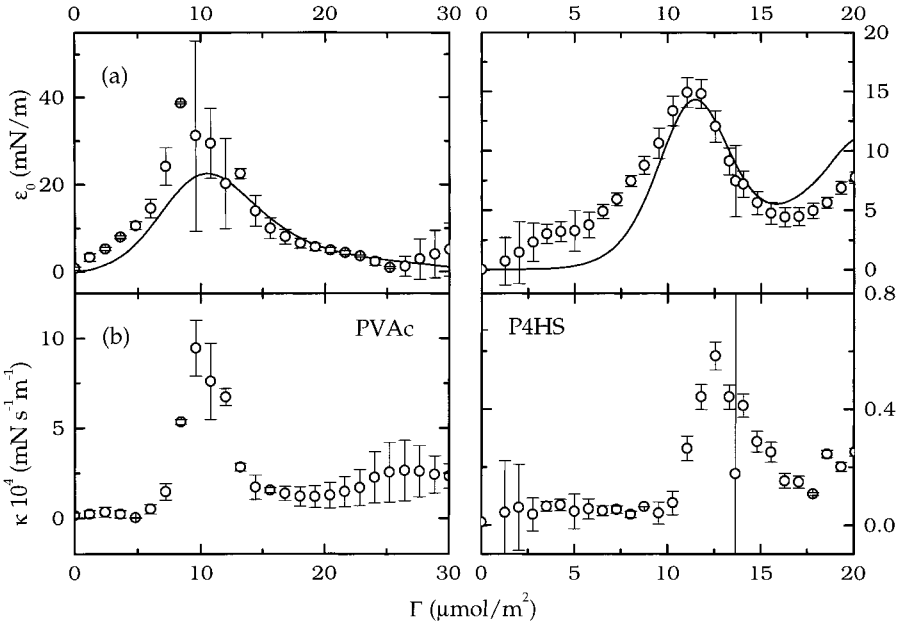

Figure 6. Dynamic elasticity $\epsilon_0(\omega)$ and dilatational viscosity $\kappa(\omega)$ for monolayers of PVAc and P4HS. The lines correspond to the static elasticity calculated from the $\Pi-\Gamma$ curves.

found it difficult to obtain reliable values of ϵ_0 and κ for monolayers of copolymers above $q = 400$ cm^{-1}.

However, as already mentioned, Buzza et al.[21] have shown that, even for thick adsorbed monolayers, $\tilde{\gamma}$ has a purely elastic character, and therefore, we have used $\mu = 0$ hereinafter. In spite that, in principle γ_0 has a Maxwell-like frequency dependence;[20] for monolayers of pure PVAc, we have found that for frequencies below 100 kHz γ_0 remains very close to the equilibrium value measured with a Wilhelmy balance.[18] The frequencies measured in the present work are below 60 kHz. In addition, the monolayers of the blends are more compressed than the one of PVAc; thus, it seems reasonable to expect that the relaxation dynamics of the transverse mode will be faster than in pure PVAc. Therefore, in this work, we have considered $\gamma_0 = \gamma_{st}$.

Figure 6 shows the values of ϵ_0 and κ obtained for the monolayers of PVAc and of P4HS. The results for the blends are similar to those shown for the pure polymers. A change of ± 0.3 mN m^{-1} in the value of γ_0 used does not change the values of κ within their estimated uncertainties.

Figure 7 shows the values of $\epsilon_0(\omega)$ calculated from ω^* and Φ^* for three of the monolayers. For comparison, it also includes the values ϵ_{st} from which one sees the parallelism with the dynamic ones; in fact, the maximum in the dilational elasticity is obtained in all cases at identical surface concentration as predicted from the static values. One can see that in the dilute and semidilute regimes, the dynamic values are slightly larger than the static ones; the difference decreases as Γ^{**} is approached. Near the collapse of the monolayers, the opposite behavior is found (see inset in Figure 7). It must be remarked that, in general, for a given value of Γ, $|\epsilon_{st} - \epsilon(\omega)|$ increases as the compressed character of the monolayer does. The qualitative tendency of ϵ_0 with x_1 is the same found from ϵ_{st}.

Figure 8 shows the composition dependence of the dilatational viscosity $\kappa(\omega)$ at different values of the surface pressure. We plot the results in this way since Π is related to the density of entanglement points δ, which plays a key role in the constitutive microscopic models used in the next section.[5] The dilatational viscosity κ increases both with x_1 and with Π (and Γ), pointing out a clear correlation between κ and Π ($\sim\delta$). The magnitude

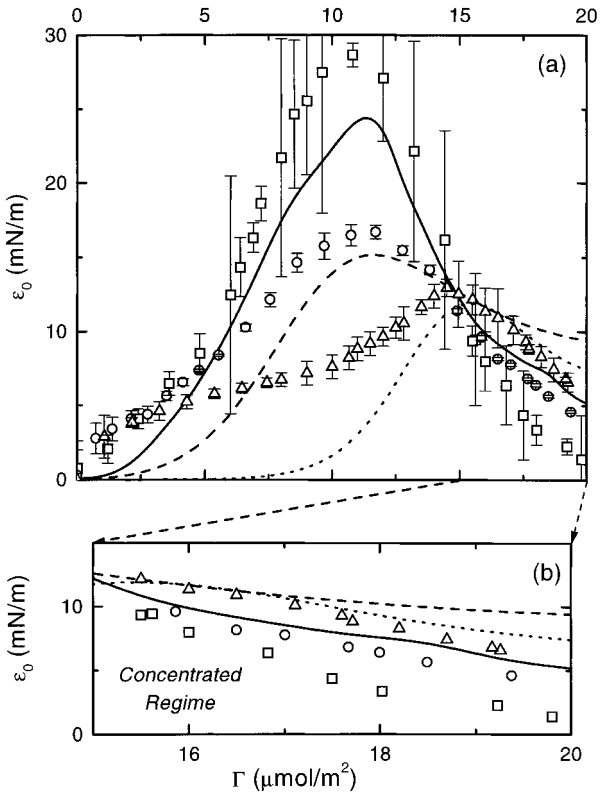

Figure 7. Dynamic elasticity modulus for some polymer blend monolayers. The symbols correspond to different values of x_1: (□) 1.0; (○) 0.75; (△) 0.25. The lines represent the corresponding values for the static elasticity modulus.

of the strong increase in κ with Π is almost independent of x_1 and therefore of chain elasticity.[2] The increase of κ with x_1 at constant Π will be discussed below. As Figure 8 points out, there is a clear parallelism between the behavior of the dilatational viscosity and the phase velocity of the transversal modes c_T. This indicates that, at least qualitatively, although the main dissipative effects upon the capillary modes in the dilute and semidilute regimes come from ϵ_0, in the concentrated regime, it is the dilational viscosity κ that essentially governs

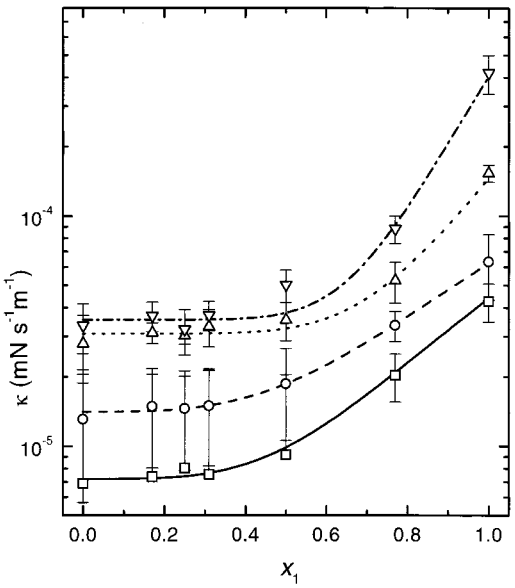

Figure 8. Dilatational viscosity coefficient for the monolayers at different values of the surface pressure. The symbols correspond to different values of Π in mN m^{-1}: (□) 0.5; (○) 1.0; (△) 5.0; (▽) 8.0. The lines aids the eye.

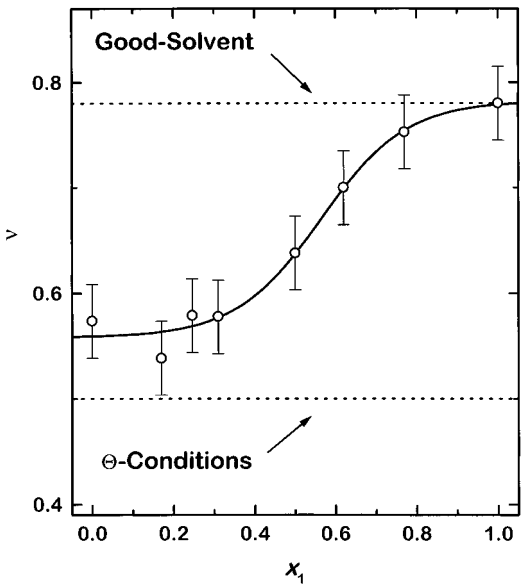

Figure 9. Flory's critical exponent as a function of blend composition. The dotted lines represent the limits for good ($\nu = 0.75$) and Θ ($\nu = 0.57$) solvent conditions.

the dissipative effects upon the propagation velocity of the transversal modes c_T ($\sim\kappa^{-1}$).

5. Discussion

It is know that the dynamics of flexible polymer chains in 3D entangled networks is well described by the reptation model.[5,36] The validity of this model rests on the real existence of two different time scales corresponding to the relaxation of an isolated polymer chain and its surroundings. In fact, in the reptation model, the viscoelastic continuum medium is assumed to relax much more slowly than a particular polymer chain diffusing in it. The crossover between these two time scales has been extensively manifested in 3-D polymer solutions, both theoretically[37] and experimentally.[38−40] However, there is comparatively less information in 2-D systems.

5.a. Semidilute Regime: Static Properties. The existence of a single characteristic length $\xi(\Gamma)$ is a crucial point for deriving scaling laws in de Gennes' theory of polymer solutions.[36] $\xi(\Gamma)$ defines the average distance between entanglement points at a monomer surface concentration, Γ, and depends on Γ, but it is independent of polymerization degree N. In a 2-D space, the density of entanglement points δ is defined as the inverse of the square of this average correlation length ξ, thus it depends explicitly on the Flory exponent ν. Hence, we can write the scaling law for δ as follows:[36]

$$\Pi \approx \delta = \xi^{-2} \approx \Gamma^{y} \tag{16}$$

which can also be written as

$$\epsilon_{st} \approx y\Pi \tag{17}$$

where $y = 2\nu/(2\nu - 1)$. Figure 9 shows the composition dependence of ν obtained from the static results. As it can be observed the interface behaves as a good solvent for monolayers rich in PVAc, while it is a near-Θ solvent for those with a significant amount of P4HS. Thus, it is reasonable to expect that the polymer coils will have expanded conformations in the interface when there is little P4HS and relatively collapsed conformations otherwise.

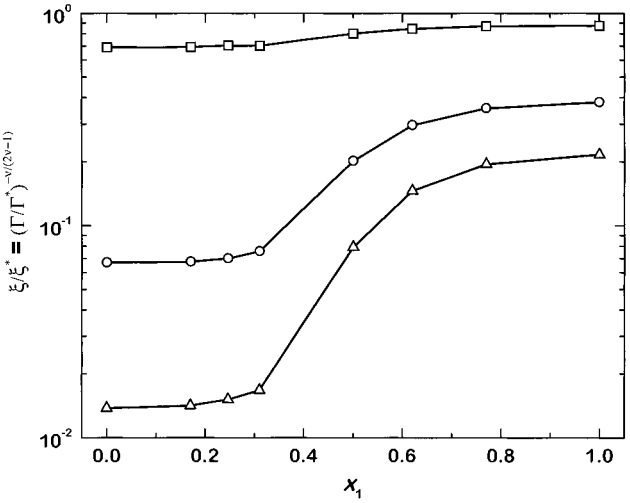

Figure 10. Dependence of the relative entanglement distance ξ on the blend composition for different values of the reduced surface concentration. Symbols represent different values of Γ/Γ*: (□) 1.1; (○) 2.0; (△) 3.0. ξ has been calculated from the experimental values of ν and Γ*.

ξ could be thus conceptually assimilated to the length of an elastic element in the polymer chain. To estimate the dimensions of ξ, one frequently calculates the hydrodynamic radius of gyration R_g, which responds to chain dimensions at overlap concentration $\Gamma^* \approx N/R_g^2$ (first contact between independent chains or dilute → semidilute transition). However, if one knows the static values of ν and Γ* (see Figure 10 and Γ* data in ref 26), it is possible to calculate the relative variation of ξ in the semidilute regime by using the scaling law given in eq 16. Figure 10 shows that ξ strongly decreases as both the content of P4HS and Γ increase.

5.b. Semidilute Regime: Dynamic Properties. Since N varies significantly between the two studied polymers ($N_{PVAc} \approx 1045$ and $N_{P4HS} \approx 85$), one can expect that R_g will increase substantially its value with x_1, varying between 4 nm for pure P4HS and 30 nm for PVAc, with this last being the maximum distance possible between entanglement points in the network. At the wave vector considered here ($q = 344.4$ cm^{-1}), the spatial scale is defined by $qR_g \leq 10^{-3} \ll 1$; thus a quasimacroscopic

continuum description of the system is satisfactory. Moreover, according to de Gennes,[36] at sufficiently low frequencies but still higher than the relaxation rate for collective reptation $\tau_R^{-1} \leq 1$ Hz, the spread monolayer is expected to behave like a gel. In this case, two parameters, the rigidity modulus of the gel E and a friction constant χ or effective viscosity of the medium, play the most significant role for the description of the system.[2] To study the time evolution of a 2-D compression mode, we will accommodate the notation of de Gennes to our constitutive parameters; in fact, the equation for the longitudinal in-plane motion can be written as:

$$\frac{\partial \Gamma}{\partial t} + \Gamma \nabla \mathbf{v} = D_s \nabla^2 \Gamma \tag{18}$$

where $\mathbf{v} = \partial \mathbf{u}/\partial t$ is the fluid velocity and D_s the surface diffusion coefficient. This equation leads to material transport at the interface, driven by surface collective diffusion, whose solutions are longitudinal modes or in-plane concentration waves of the form

$$\Gamma(x;t) = \Gamma_0 + \Gamma_1(t) = \Gamma_0 + \delta\Gamma e^{iqx} e^{i\omega t} \tag{19}$$

Since the tangential stress does go given by in plane compression−expansion processes (dilational elastic stress), which takes place thanks to surface tension gradients, the stress−strain relation for this motion is[16,22,41]

$$\frac{d\gamma}{dx} = \tilde{\epsilon}(\omega) \frac{\partial^2 \mathbf{u}_x}{\partial x^2} \tag{20}$$

Substitution in eq 18 and solving for the longitudinal mode in eq 19, one obtains diffusive modes $\Gamma(t) \approx \exp(-t/\tau_D)$, where the relaxation time τ_D is

$$\tau_D^{-1} = D_s q^2 \tag{21}$$

which governs a Maxwell-like viscoelastic relaxation for the dilational modulus:[20]

$$\tilde{\epsilon}(\omega) = \epsilon_{st} + \epsilon_\infty \frac{(\omega\tau_D)^2 + i\omega\tau_D}{1 + (\omega\tau_D)^2} \tag{22}$$

According to the arguments from de Gennes and if the hydrodynamic interactions between monomers are taken into account, the dynamic properties follow a scaling behavior governed by the correlation length ξ, having the following scale laws in the case of a space of dimensionality $d = 2$:[2]

$$\tau_D^{-1} \approx \xi^{-1/\nu} \approx \Gamma^{1/(2\nu-1)}$$

$$\epsilon_0 \approx \xi^{-2} \approx \Gamma^{2\nu/(2\nu-1)} \tag{23}$$

$$\kappa \approx \xi^{-(2\nu+1)/\nu} \approx \Gamma^{(2\nu+1)/(2\nu-1)}$$

To verify the validity of the dynamic laws given in eqs 23, we should be able to correlate the observed high-frequency dynamic behavior using the equilibrium values of ξ, previously calculated.

Figure 11 shows the experimental values of the dilatational viscosity for the two pure polymers for $q = 344.4$ cm^{-1}. In both cases, κ displays a plateau at low surface concentrations, beginning to grow suddenly in the semidilute regime. From linear fits in the double log−log representation, we have calculated its scale exponent y, obtaining 4.18 ± 0.13 and 14.2 ± 1.7 for PVAc and P4HS, respectively. These values are in excellent agreement with the expected ones from the expression given in eq 23 and the values of the Flory exponent obtained from the $\Pi-\Gamma$ curves (see Figure 9). Figure 12 shows the scaling exponents (eq 23) for $\epsilon_0(\omega)$ and $\kappa(\omega)$ in the semidilute regime as a function of blend composition. It also includes the predictions using the values of ν obtained from the static data. The agreement between the values obtained from static and dynamic properties is excellent for all the systems studied. This confirms the consistency of static and dynamic data with the scaling laws for polymer monolayers in the semidilute regime for systems ranging from good to Θ solvents.

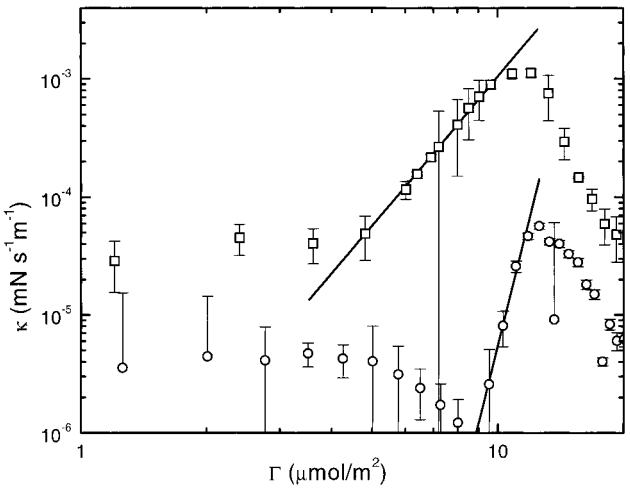

Figure 11. Surface concentration dependence of the dilatational viscosity for the monolayers of the pure polymers: (□) PVAc; (○) P4HS. The straight lines represent the scaling behavior predicted for the semidilute regime, eq 24.

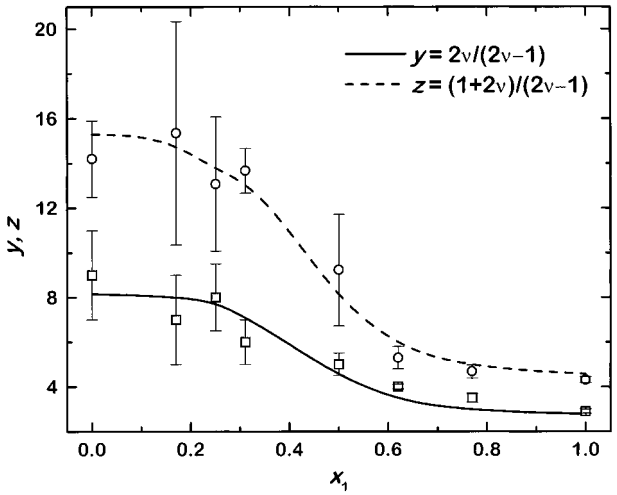

Figure 12. Blend composition dependence of the scaling laws exponents for the dynamic elasticity modulus and dilatational viscosity in the semidilute regime (eq 24). The lines are the predictions obtained with the value of ν obtained from the static elasticity modulus.

The results shown in Figure 10 are apparently in conflict with the predicted dynamic scaling behavior. In effect, eq 23 leads to a decrease of ϵ_0 and κ when ξ increases. However the comparison of Figures 8 and 10 shows that κ and ξ increase simultaneously as x_1 increases. This apparent inconsistency is caused by the use of de Gennes's theory for all the monolayers. In fact, the theory, as outlined, is strictly valid only if the chains behave as an expanded elastic element with $\nu = 0.75$ for $d = 2$. Therefore, the dynamic scale arguments will remain ap-

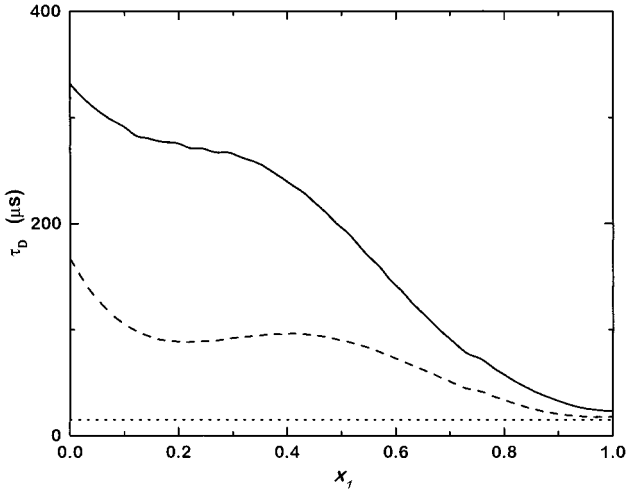

Figure 13. (a) Relaxation time for collective longitudinal modes at $q = 344.4$ cm^{-1} as a function of blend composition and for different values of Π in mN m^{-1}: (—) 0.5; (---) 1.0; (···) 3.0.

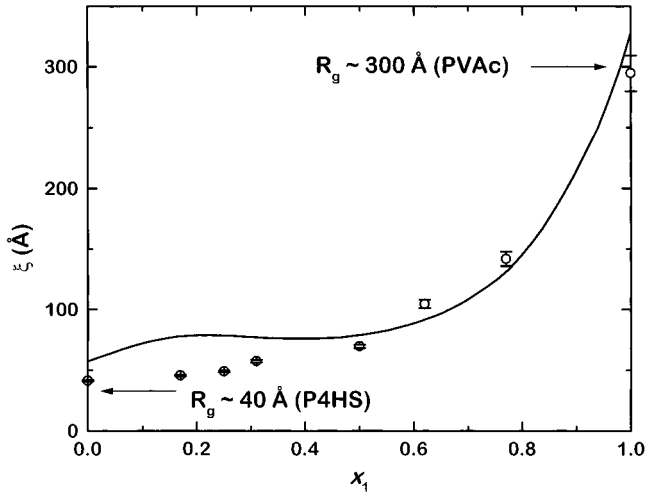

Figure 14. Comparison of the entanglement length calculated from the static overlaping concentration Γ* (points) and from the dynamic elasticity modulus ϵ_0 at 1 mN/m (line).

plicable only if $\nu \rightarrow 0.75$, i.e., far from Θ conditions. As was already said, this situation corresponds only to PVAc-rich monolayers.

A qualitative picture that can emerge from the above dynamic results in the semidilute regime is that the P4HS coils act as small rigid-like filling elements within the PVAc matrix. These elements will contribute to increase ξ in the entangled network of extended PVAc chains. If we use an effective distance between entanglement points ξ_{eff} proportional to $1 - x_1$, ξ_{eff} will start to depart from ξ value at distances below the hydrodynamic radius of the P4HS ($\xi \leq 40$ Å). It is important to emphasize that this distance corresponds to concentrations of 100 μmol m^{-2} in the pure PVAc monolayer, being however larger than the characteristic distance between entanglement points in the pure P4HS monolayer at Γ*. This would make it necessary to introduce a prefactor in eq 23 which accounts for this effects.

Using eq 22 and the experimental values of the viscoelastic coefficients shown in Figure 8 for $\Gamma < \Gamma^{**}$, we have calculated the dilational relaxation time τ_D as the ratio of the imaginary and real components of $\tilde{\epsilon}$. As can be observed in Figure 12, for low values of Π, τ_D decreases as x_1 increases while it remains almost constant for values of Π larger than 3 mN m^{-1}.

According to de Gennes, for the semidilute regime and $q\xi \ll 1$, τ_D can be written as[2]

$$\tau_D^{-1} = \frac{E}{\eta_s}(q\xi)^2 \approx \frac{\epsilon_0}{H\eta_s}(q\xi)^2 \qquad (24)$$

where E is the elastic modulus for a 3-D gel and η_s the viscosity of the subphase. E can be estimated as $E \approx \epsilon_0/H$, with H being the depth of the interfacial layer. Using ellipsometry data, Sauer et al.[42] have calculated $H = (6.0 \pm 0.5)$ Å for monolayers of PVAc. Assuming the same value of H for all the blend compositions in the semidilute regime, we have calculated ξ from the values of τ_D shown in Figure 13. Figure 14 shows the values of ξ from the dynamic elasticity coefficient ϵ_0 for $\Pi = 1$ mN/m together with the values calculated from the overlapping concentration Γ* obtained from the equilibrium Π−Γ curves. The agreement is good, considering the approximations involved in eq 24. These results represent, on one side, a further test of the consistency between the static and dynamic properties obtained from the capillary wave spectroscopy and on the other side agree with de Gennes' picture that describes the semidilute monolayer as a 2-D gel.

5.c. Concentrated Regime. Figure 7 shows that for $\Gamma > \Gamma^{**}$ the dynamic values of $\epsilon_0(\omega)$ are lower than the static ones. In addition, in this concentration range $\kappa(\omega)$ decreases as Γ increases. In fact, this tendency of $\kappa(\omega)$ to vanish as Γ increases in the concentrated regime is a general feature in polymer monolayers with partially charged or dipolar functional groups. These facts seem incompatible with the absence of tridimensional diffusional exchange with the bulk phases as is the case of completely insoluble monolayers.[41,43] Therefore, they suggest the apparition of well-defined loops and/or tails of the polymer chain protruding in either adjacent phase, accommodating in this way the excess of monomer concentration with regard to the adsorption sites onto the surface. Low−frequency mechanical experiments performed in pure PVAc monolayers have evidenced the existence of a rich reptation dynamics associated with this out-of-plane segments of the polymer chains,[18] compatible with the theoretical model of Noskov.[44]

A simple way of taking into account diffusive processes from/to the interface plane is provided by the Lucassen−van den Tempel formalism for adsorbed monolayers.[31,41,43] Despite that this theory was originally developed for soluble surfactants, the theoretical frame can be tentatively extended to spread films if, in lieu of the diffusion process from the bulk to the surface, we now invoke an analogous process in the z-direction, which responds to the diffusive transport of the polymeric material in the transversal direction (adsorption/desorption of loops and tails in Noskov's theory[44]). This diffusion is driven by a certain packaging density distribution $c(\Gamma;z)$ of the polymer chains (see also eqs 28 and 29). This conceptual extension has been successfully applied to explain certain dynamic features of insoluble monolayers of small molecules such as long-chain alcohols and acids.[45]

Briefly, if the steady state is assumed between the polymer concentration at the interface Γ (number of 2-D adsorption sites per area) and the 3-D distribution $c(\Gamma;z)$ in the adjacent bulk phases, and one supposes diffusive transport through this 3D package, characterized by an internal diffusion coefficient D_c, which will depend on chain structure and hydrodynamic interactions with the solvent, in this case, the modified Lucassen−van den Tempel model yields a viscoelastic behavior given by[45]

$$\frac{\tilde{\epsilon}(\omega)}{\epsilon_{st}} = \frac{\epsilon_0(\omega) + i\omega\kappa}{\epsilon_{st}} = \frac{(1+\Omega) + i\Omega}{2\Omega^2 + 2\Omega + 1} \tag{25}$$

where Ω is a reduced frequency defined by

$$\Omega = \sqrt{\frac{D_c}{2\omega}}\frac{dc}{d\Gamma} = \sqrt{\frac{1}{\omega\tau_c}} \tag{26}$$

It is worth noting that D_c responds to a diffusive-like transport in the thinned polymer film, driven by a certain concentration gradient which responds to the *z*-dependent packaging distribution $c(\Gamma;z)$. In this case, the mass conservation leads to the ordinary Fick diffusion equation, $\partial c/\partial t = D_c\nabla^2 c$.

Obviously, if these assumptions were also valid in the concentrated regime, Ω may be calculated from these equations by using the experimental values of ϵ_0 and κ in this regime:

$$\frac{\epsilon_0}{\omega\kappa} = \frac{1+\Omega}{\Omega} \tag{27}$$

Figure 15 shows τ_c for the blends at three values of Π. It can be observed that τ_c decreases as Π (or Γ) increases, although such a dependence vanishes for monolayers rich in PVAc. It must be noticed that the values of τ_c are almost 10 fold those of τ_D. This means that the dynamics of the material in the volume immediately beneath the surface (monolayer) is slower than that in the monolayer. This can be understood by considering that τ_c reflects the reorganization of long tails and/or loops of the polymer chains immersed in the subphase, where the gain of a degree of freedom with respect to the interface involves the relaxation of extra molecular motions.

However, the explanation of the existence of maxima in some of the curves of Figure 15 is not straigtforward since, as discussed previously, the quality of the interface as solvent of the blends changes monotonically from pure PVAc to pure P4HS. To further discuss these findings, it is necessary to consider that in the concentrated regime the polymer chain has three types of segments: the so-called trains that are adsorbed in the 2-D interface and the loops and the tails that are immersed in the subphase.[44] Equation 26 clearly shows that τ_c strongly depends on the equilibrium magnitude $d\Gamma/dc$, which in turn is determined by the concentration profile through the interface. To describe this situation, one may resort to the concentration profile proposed a few years ago by de Gennes[46] and recently tested against polymer adsorption results by Klein and Rossi.[47]

$$\varphi(z) = \left(\frac{a}{\frac{3}{4}\xi_{loop} + z}\right)^{4/3} \tag{28}$$

with *z* being the distance to the surface from the bulk liquid, φ being the volume fraction, and ξ_{loop} reflecting the size of the elastic loops/tails under the monolayer. It is possible to relate φ with the mass fraction *c* through a mass density factor *S* such that

$$c(z) = S\varphi(z) \tag{29}$$

S represents the density of monomers within a loop/tail, thus being a function of $\Pi(\Gamma)$. According to the concentration profile proposed by de Gennes,[46] it is possible to write

$$\tau_c \approx \left(\frac{\xi_{loop}}{S}\right)^2 \tag{30}$$

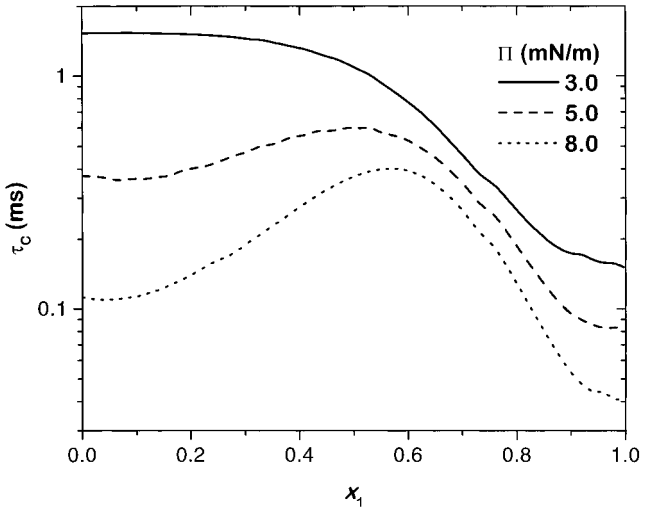

Figure 15. Relaxation time calculated from the Lucassen−van den Temple model for the concentrated regime at different surface pressures.

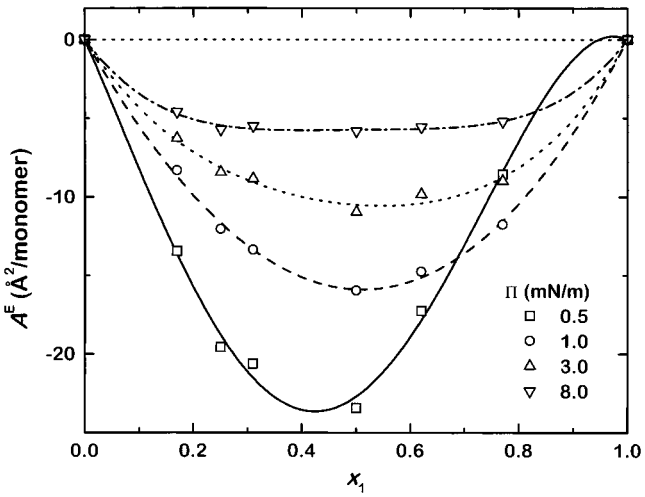

Figure 16. Excess area for the PVAc + P4HS blend as a function of composition for different surface pressures.

Equation 30 will allow us to discuss *qualitatively* the results shown in Figure 15. In effect, for low values of Π (which for a given blend correspond to low values of Γ), one may expect that *S* will be small and will not change appreciably with blend composition and hence τ_c will depend essentially on ξ_{loop}. Under these conditions, one may expect that ξ_{loop} will be lower for an interface that behaves as a good solvent for the polymer (PVAc-rich blends) than when it is a near-Θ solvent (P4HS-rich blends).[48] This is the behavior observed for $\Pi = 3$ mN/m in Figure 16.

High values of Π correspond to high values of Γ for a given blend and it must be expected that also to larger values of *S*. The decrease of τ_c with increasing Π indicates (eq 31) that the increase of ξ_{loop} with Π (if any) is smaller than that of *S*. The change of *S* with blend composition will be related to the ability of the monolayer to store polymeric material. A qualitative idea of such an ability is given by the excess area A^E of the monolayer shown in Figure 16 and which is obtained as a difference between the inverse of the actual surface concentration and the ideal contribution at a given pressure, $A^E = (1/\Gamma) - x_1\,(1/\Gamma_1) - x_2\,(1/\Gamma_2)$. As it can be observed, A^E is strongly negative, with a minimum near $x_1 = 0.5$. The minimum becomes less pronounced as Π increases and shifts toward lower concentrations of PVAc. This minimum will correspond to a maximum density in the monolayer and thus to lower values

of S as Π increases. As it can be observed the Π and x_1 trends of τ_c and A^E are well correlated.

6. Conclusions

Static surface pressure and elasticity results have been obtained for monolayers of PVAc + P4HS blends over the whole surface concentration and blend composition ranges. The results corresponding to the semidilute regime have been analyzed in terms of scaling laws. The values of the critical exponent ν point out that the aqueous−air interface is a good solvent for PVAc-rich monolayers and a near-Θ solvent for P4HS-rich ones. For a given value of Π, the entanglement distance ξ increases with the content of P4HS in the blend. For a given blend, ξ decreases with Π as expected.

The viscoelastic coefficients corresponding to the longitudinal mode have been estimated from the analysis of the correlation functions corresponding to the light scattered by the capillary waves. In the semidilute regime, the analysis of the dilatational viscosity and of the dynamic elasticity in terms of scaling laws lead to critical exponents that are in excellent agreement with those obtained from the static properties.

In the concentrated regime, the dynamic values of the elasticity are lower than the static ones for all the systems studied. This suggests the existence of out-of-plane diffusion processes, through which tails and loops of the polymer chains protrude into the adjacent phases, a picture similar to that described recently by Noskov.[44] The dynamics of these reptation processes is characterized by frequencies lower than those used in the present study.

Acknowledgment. This work was supported in part by Fundación Ramón Areces, and by DGES under grant PB96-609. F. Monroy thanks UCM for a FPI fellowship.

References and Notes

(1) Ferry, J. D. *Viscoelastic Properties of Polymers*; John Wiley & Sons: New York, 1980.
(2) de Gennes, P. G. *Macromolecules* **1976**, *9*, 587; **1976**, *9*, 594.
(3) Rouse, P. E. *J. Chem. Phys*. **1953**, *21*, 1272.
(4) Doi, M.; Edwards, S. F. *J. Chem. Soc., Faraday Trans. 2* **1978**, *74*, 1789.
(5) Doi, M.; Edwards, S. F. *The Theory of Polymer Dynamics*; Clarendon Press: Oxford, 1986.
(6) Buhaenko, M. R.; Richardson, R. M. *Thin Solid Films* **1988**, *159*, 231.
(7) Landau, L. D.; Lifshitz, E. M. *The Theory of Elasticity*; Pergamon Press: Oxford, 1986.
(8) Edwards, S. F. *Proc. Phys. Soc. London* **1967**, *95*, 513.
(9) Kawaguchi, M. *Prog. Polym. Sci.* **1993**, *18*, 341.
(10) Kramer, L. *J. Chem. Phys.* **1971**, *55*, 2097.
(11) Fan, C. *J. Colloid Interface Sci.* **1972**, *44*, 369.
(12) Goodrich, F. C. *Proc. Royal. Soc. London A* **1981**, *374*, 341.
(13) Nelson, D. R.; Halperin, B. I. *Phys. Rev. B* **1979**, *19*, 2457.
(14) Maru, H. C.; Wasan, D. T. *Chem. Eng. Sci.* **1979**, *34*, 1295.
(15) Monroy, F.; Kahn, J.; Langevin, D. *Colloids and Surfaces* **1998**, *143*, 251.
(16) Langevin, D., Ed. *Light Scattering by Liquid Surfaces and Complementary Techniques*; Surfactant Science Series 41; Dekker: New York, 1992.
(17) Kikuchi, H.; Sakai, K.; Takagi, K. *Phys. Rev. B.* **1994**, *49*, 3061; *Jpn. J. Appl. Phys.* **1991**, *30*, L1668.
(18) Monroy, F.; Ortega, F.; Rubio, R. G. *Phys. Rev. E* **1998**, *58*, 7629.
(19) Earnshaw, J. C.; McGivern, R. C.; Winch, P. J. *J. Phys. (France)* **1988**, *49*, 1271.
(20) Harden, J. L.; Pleiner, H. *Phys. Rev. E* **1994**, *49*, 1411.
(21) Buzza, D. M. A.; Jones, J. L.; McLeish, T. C. B.; Richards, R. W. *J. Chem. Phys.* **1998**, *109*, 5008.
(22) Levich, V. G. *Physicochemical Hydrodynamics*; Prentice Hall: New Jersey, 1962.
(23) Earnshaw, J. C.; McGivern, R. C. *J. Phys. D: Appl. Phys.* **1987**, *20*, 82.
(24) Jasper, J. J. *J. Phys. Chem. Ref. Data* **1972**, *1*, 841.
(25) Richards, R. W.; Rochford, B. R.; Taylor, R. M. *Macromolecules* **1996**, *29*, 1980.
(26) Yoo, K. W.; Yu, H. *Macromolecules* **1989**, *22*, 4019.
(27) Richards, R. W.; Taylor, M. R. *J. Chem. Soc., Faraday Trans.* **1996**, *92*, 601.
(28) Monroy, F.; Ortega, F.; Rubio, R. G. *Colloids Polym. Sci.* **1998**, *276*, 960.
(29) Garrett, W. D.; Zisman, W. A. *J. Chem. Phys.* **1969**, *74*, 1796.
(30) Runge, F. E.; Yu, H. *Langmuir* **1993**, *9*, 3191.
(31) Lucasen, J.; van den Tempel, M. *J. Colloid Interface Sci.* **1972**, *41*, 491.
(32) Kawaguchi, M.; Sauer, B. B.; Yu, H. *Macromolecules* **1989**, *22*, 1735.
(33) Earnshaw, J. C.; McLaughlin, A. C. *Proc. R. Soc. London Ser. A* **1993**, *430*, 519.
(34) Peace, S. K.; Richards, R. W.; Williams, N. *Langmuir* **1998**, *14*, 667.
(35) Peace, S. K.; Richards, R. W. *Polymer* **1996**, *37*, 4945.
(36) de Gennes, P. G. *Scaling Concepts in Polymer Physics*; Cornell University Press: Ithaca, NY, 1979.
(37) Szleifer, I.; Loring, R. F. *J. Chem. Phys.* **1991**, *95*, 2080.
(38) Graessley, W. W. *Adv. Polym. Sci.* **1982**, *47*, 68.
(39) Watanabe, H.; Tirrell, M. *Macromolecules* **1989**, *22*, 927.
(40) Hess, W. *Macromolecules* **1988**, *21*, 2620.
(41) Lucassen-Reynders, E. H.; Lucassen, J. *Adv. Colloid Interface Sci.* **1969**, *2*, 347.
(42) Sauer, B. B.; Yu, H.; Yazdanian, M.; Zografi, G.; Kim, M. M. *Macromolecules* **1989**, *22*, 2332.
(43) Lucassen, J.; van den Tempel, M. *Chem. Eng. Sci.* **1972**, *271*, 1283.
(44) Noskov, B. A. *Colloid Polym. Sci.* **1995**, *273*, 263.
(45) Cini, R.; Lombardini, P. P.; Manfredi, C.; Cini, E. *J. Colloid Interface Sci.* **1987**, *119*, 1.
(46) de Gennes, P. G. *Macromolecules* **1981**, *14*, 1637.
(47) Klein, J.; Rossi, G. *Macromolecules* **1998**, *31*, 1979.
(48) Joanny, J.-F.; Johner, A.; Rubinstein, M. *Colloids Surf. A* **1994**, *86*, 133.